INSTITUTE OF PHYSICS PUBLISHING SUPERCONDUCTOR SCIENCE AND TECHNOLOGY

Supercond. Sci. Technol. **18** (2005) 1100–1105 doi:10.1088/0953-2048/18/8/013

A high temperature superconductor tape RF receiver coil for a low field magnetic resonance imaging system

M C Cheng, B P Yan[1], K H Lee, Q Y Ma and E S Yang

Jockey Club MRI Centre, The University of Hong Kong, Hong Kong SAR, People's Republic of China

E-mail: bpyan@eee.hku.hk

Received 11 March 2005, in final form 23 May 2005
Published 5 July 2005
Online at stacks.iop.org/SUST/18/1100

Abstract

High temperature superconductor (HTS) thin films have been applied in making a low loss RF receiver coil for improving magnetic resonance imaging image quality. However, the application of these coils is severely limited by their limited field of view (FOV). Stringent fabrication environment requirements and high cost are further limitations. In this paper, we propose a simpler method for designing and fabricating HTS coils. Using industrial silver alloy sheathed $Bi_{(2-x)}Pb_xSr_2Ca_2Cu_3O_{10}$ (Bi-2223) HTS tapes, a five-inch single-turn HTS solenoid coil has been developed, and human wrist images have been acquired with this coil. The HTS tape coil has demonstrated an enhanced FOV over a six-inch YBCO thin film surface coil at 77 K with comparable signal-to-noise ratio.

(Some figures in this article are in colour only in the electronic version)

1. Introduction

Magnetic resonance imaging (MRI) is a powerful tool in contemporary medical diagnostics. The image quality of clinical MRI depends crucially on the signal-to-noise ratio (SNR) available from the MRI system [1]. In a MRI system, what is used to detect the weak MR signal radiated from a biological sample is a RF receiving coil, the SNR of which determines the quality of the MRI image. Degradation of the image mainly arises from two noise sources. One is the thermally induced Johnson noise arising from the imaged sample and the other is Johnson noise from the RF receiving coil. During imaging, the loss from biological samples can be coupled to the RF coil. Thus, the SNR of the MRI system can be expressed as [2]

$$\mathrm{SNR} \propto \frac{B_1}{\sqrt{R_c T_c + R_s T_s}} \tag{1}$$

where B_1 is the magnetic field produced by the coil per unit current when used as the transmission coil. R_c and T_c are the coil resistance and temperature, respectively. R_s and T_s are the sample resistance coupled to the RF coil and sample temperature, respectively. From expression (1), clearly, it is necessary to reduce the noise figure of an MRI system to boost the SNR. In high field MRI systems, the biological sample noise dominates the total noise content [1]. Thus, an improvement in the noise figure of the receiver electronics will not improve the SNR of the image at the frequency of operation. However, as the size of the sample to be imaged and receiving coil are reduced, the RF coil noise will eventually become predominant. In this case, it is possible to enhance the SNR by reducing the coil noise. We have done so by using $Bi_{(2-x)}Pb_xSr_2Ca_2Cu_3O_{10}$ (Bi-2223) high temperature superconductor (HTS) tape.

Although HTS thin film coils with different sizes have been applied in high field (>4 T) microscopy [1–3] and low field peripheral human anatomy imaging [4–6], there are still some problems in clinical practice for human imaging due to the following limitations. First, HTS thin film coils are usually formed on $LaAlO_3$ or sapphire substrates [7]. The flat and rigid nature of the substrate limits the coil configuration to planar geometry. Since HTS thin film coils only image a superficial region of the sample, their field of view (FOV) is

[1] Author to whom any correspondence should be addressed.

very limited and, furthermore, they also suffer from a quick drop in signal intensity as a function of distance from the surface of the coil [8]. Second, the filling factor (η), which is defined as the fraction of RF energy created by the coil, is related to SNR by [9]

$$\mathrm{SNR} \propto \sqrt{\eta Q}. \tag{2}$$

To maximize the filling factor, it is desirable to have the RF coil wrap around the sample so that more nuclear magnetic dipoles can contribute to the signal. Since the filling factor of HTS thin film coils is much smaller than that of a volume coil, for maintaining sufficient thermal insulation, the SNR improvement offered by HTS cannot be fully realized for thin film coils [9]. Third, HTS thin film coils require a stringent clean room fabrication environment and microfabrication expertise, which causes some inconvenience in coil fabrication. In this paper, we have proposed a simpler and easier method for designing and fabricating HTS coils. Using industrial silver alloy sheathed $Bi_{(2-x)}Pb_xSr_2Ca_2Cu_3O_{10}$ (Bi-2223) HTS tapes [10, 11], a high quality RF HTS volume coil is realized and human wrist images have been acquired. The fabricated HTS tape volume coil has demonstrated an enhanced FOV over a six-inch YBCO thin film surface coil at 77 K with comparable SNR. The realization of a HTS tape volume coil enables the application of HTS in scanning deep lying organs or extremities.

2. Theory

In this model, we aim at predicting the theoretical SNR gain offered by the HTS tape coil over an equivalent copper and silver coil at different temperatures (77 and 300 K). Using equation (1), the theoretical SNR gain can be estimated using

$$\frac{\mathrm{SNR}_{(\mathrm{tape})}}{\mathrm{SNR}_{(\mathrm{Cu/Ag})}} = \frac{\sqrt{R_{(\mathrm{Cu/Ag})}T_{(\mathrm{Cu/Ag})} + R_sT_s}}{\sqrt{R_{(\mathrm{tape})}T_{77\ \mathrm{K}} + R_sT_s}} \tag{3}$$

where R and T stand for resistance and temperature, respectively. The subscripts (tape), (Cu), (Ag) and (s) denote the HTS tape, copper, silver coil and the imaged sample. In the deduction of (3), we have assumed that (i) all coils have the same sensitivity profile B_1 and the same geometry; and (ii) the pre-amplifier noise is negligible compared to the coil noise and sample noise.

The resistance R_c of a RF coil at resonant angular frequency ω_0 can be found from the unloaded quality factor (Q_{unloaded}):

$$R_c = \frac{L\omega_0}{Q_{\mathrm{unloaded}}} \tag{4}$$

where L is the inductance of the coil. Besides the coil resistance, the imaging sample will also couple loss to the receiver coil. The sample resistance R_s coupled to the coil can be estimated from

$$R_s = \frac{L\omega_0(Q_{\mathrm{unloaded}} - Q_{\mathrm{loaded}})}{Q_{\mathrm{unloaded}}Q_{\mathrm{loaded}}}. \tag{5}$$

The inductance of the HTS tape and copper coil can be deduced from the capacitance C and the resonant frequency f:

$$L = \frac{1}{C(2\pi f)^2}. \tag{6}$$

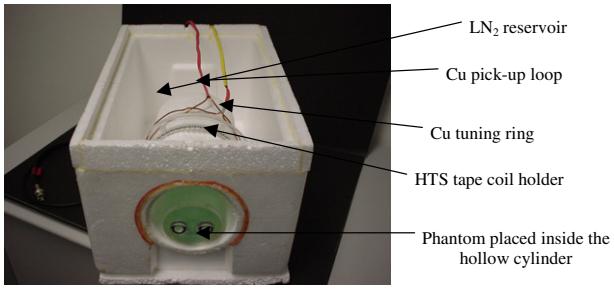

Figure 1. Styrofoam cryostat with a coil holder, tuning ring and pick-up loop.

3. Material and methods

3.1. HTS tape coil fabrication

The Bi-2223 high current density wire was purchased from American Superconductor Corp. (Westborough, MA) with thickness of 0.21(±0.02 mm) and width of 4.1(±0.2 mm) [12]. The pre-modified tape has an outer Ag alloy layer of thickness (∼40 μm) to improve the mechanical strength. When it is used to pick up MR signals in the MHz range, current will flow predominantly in the outside cross-section of the conductor due to the skin effect. Taking the conductivity of silver based alloy (chemically compatible with Bi-2223 phase) at 77 K, the skin depth is about 10.7 μm at 8.92 MHz. Therefore, the silver sheath has been completely removed by chemical wet etching [14] to prevent screening out the RF signal from the superconducting phase. High Q capacitors are soldered with the HTS tape to obtain the desirable resonant frequency.

3.2. HTS tape coil holder and cryostat design

An acrylic coil holder was designed in order to (i) provide the necessary mechanical support; (ii) sustain a low temperature (77 K) without serious contraction; and (iii) ensure chemically inertness to the etching solution. The coil holder was made into a circular shape to make it more resistant to thermal cracking. Also, it has a circular groove to hold the coil in shape and to ensure effective cooling and etching.

Figure 1 shows the cryostat which was made using Styrofoam. The HTS tape coil (placed inside the coil holder) is wound around the hollow cylinder and cooled by liquid nitrogen (LN_2). The imaged sample is accommodated inside the cylinder with a coil-to-sample separation of about 2 cm. As shown in figure 1, to preserve the SNR of the superconducting coil, the signal received is inductively coupled [13] to a copper pick-up loop, which is connected to a standard GaAs MESFET pre-amplifier at room temperature. The size of the pick-up loop is identical to the tape coil for optimized SNR inductive coupling. The resonant frequency of the tape coil is fine-tuned by a movable copper tuning ring. Both the tuning ring and pick-up loop are placed inside the LN_2 bath to reduce the thermal noise coupled to the low loss HTS tape coil.

3.3. Copper and silver coil

For comparison with the HTS tape coil, equivalent copper and silver coils were also fabricated. The equivalent copper coil

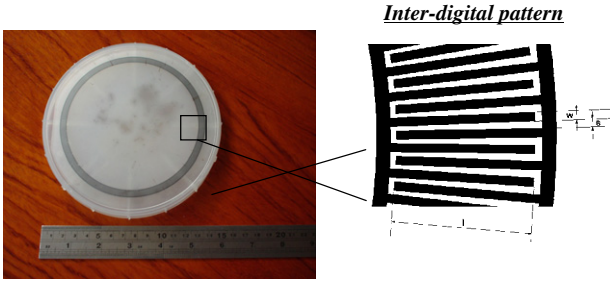

Figure 2. HTS thin film surface coil made of six-inch YBCO thin film. The mean diameter of the coil pattern is 5.5″.

was made with 3M copper tapes and high Q capacitors and the silver coil was fabricated with 96% purity silver tape with a rectangular cross-section of 3 mm × 1 mm and soldered with high Q capacitors.

3.4. HTS thin film surface coil and cryostat

A HTS surface coil was fabricated with a six-inch YBCO thin film deposited on a sapphire substrate. As shown in figure 2, an interdigitated pattern was formed on the wafer by a photolithography and etching technique [7]; it carries a resonant frequency of 8.8 ± 0.1 MHz. Figure 3 shows the cryostat for the HTS film surface coil which is made of Styrofoam and fibre reinforced plastic (FRP). The cryostat contains a copper tuning plate for fine frequency tuning and a pick-up loop for signal pick-up and matching to the pre-amplifier. The separation between the coil and sample is 2 cm.

3.5. Q value measurement

The Q values of the coils were measured by the Hewlett-Packard 8753E Network Analyzer using the dual coupling technique [13]. Values are taken both outside the magnet and at the iso-centre of a home-built 0.21 T MRI system. To represent the loaded condition, a cylindrical phantom (diameter 2.5″ × height 6″) filled with 3.3 g l^{-1} $CuSO_4$ solution or the wrist of a healthy volunteer was inserted through the RF coil.

3.6. Imaging experiment

Phantom and human wrist images were acquired using our home-built 0.21 T (8.92 MHz) MRI scanner. The magnet and gradient coils were made in the Chinese Academy of Sciences, the gradient control and power amplifier were from Copley Control Corp. (Canton, MA), the console was from Tecmag, Inc. (Houston, TX) and we used an in-house-designed user interface. The gradient strength is 20 mT m^{-1}, the power of the RF amplifier is 300 W and the console is run on a Pentium IV 2.4 GHz PC. All the RF coils are decoupled from the transmission coil by orthogonal placement. All images were obtained with a conventional spin-echo pulse sequence with (TR/TE = 400/31 ms, NEX = 2, FOV = 18 cm × 18 cm, matrix size = 256 × 256, slice thickness = 5 mm and acquisition bandwidth 12 kHz) in approximately 3.5 min. Images were reconstructed and analysed using locally written IDL analysis tools (Research Systems, Inc., Boulder, CO).

3.7. SNR profile

The SNR profile of an RF coil along its central axis is given by

$$\mathrm{SNR} = \frac{\mathrm{Signal}_{(\mathrm{mean})} - \mathrm{Noise}_{(\mathrm{mean})}}{\mathrm{Noise}_{(\mathrm{S.D.})}}.$$

With phantom images (sagittal view) taken, the mean signal intensity along the coil's central axis was smoothed within a window of four pixels. The noise mean and standard deviation were measured with rectangular ROIs drawn on the background.

4. Results and discussion

4.1. Quality factor and coil resistance

The quality factor and resistance of coils made of HTS tape, silver, copper were measured at different temperatures and the results are summarized in table 1 (inside magnet) and table 2 (outside magnet). The coil resistance was calculated by reference to the Q values and using equations (4)–(6). All RF coils show an increase in resistance when they are placed inside the magnet. For the RF coil made of normal metal (i.e. copper and silver), the additional resistance was mainly contributed by the conductor inside the MRI system (e.g. gradient coils, transmission coil, shimming coil). We found that the coupled loss was about 2–3 mΩ, which is comparable to the sample resistance of the phantom (2 mΩ) and wrist (2.2 mΩ). For the HTS tape RF coil, the resistance was increased significantly, about three times, to 12.5 mΩ. Besides the aforementioned conductor loss, as we may expect from all HTS RF coils, the magnetic field will also cause the rapid formation of magnetic vortex structure [15] inside the HTS material, which will increase the resistance significantly.

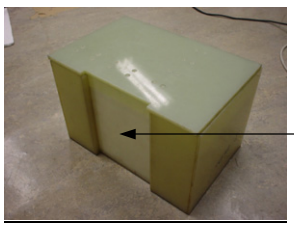

Figure 3. Cryostat for the HTS thin film surface coil.

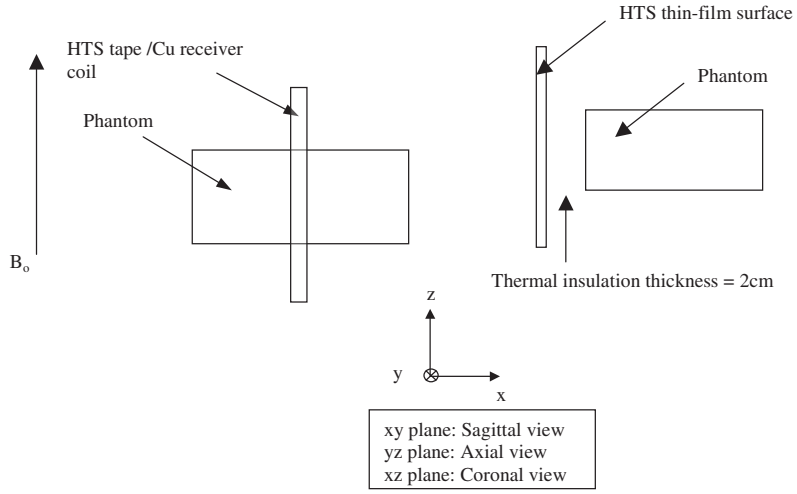

Figure 4. The coil and sample position inside the 0.21 T system (the cryostat is shown in this diagram).

Table 1. Quality factor and coil resistance comparison (at the 0.21 T magnet iso-centre).

Tuned at 8.92 MHz (at 0.21 T magnet iso-centre).						
Coil type/ temperature	Diameter (inch)	Inductance L (μH)	Unloaded Q	Coil resistance R_c (mΩ)	Loaded Q (phantom)	Loaded Q (wrist)
HTS tape@77 K	5″	0.31	866	20.0	788	780
Cu@77 K	5″	0.32	264	68.0	262	250
Ag@77 K	5″	0.31	168	104.1	160	152
Cu@300 K	5″	0.25	131	136.9	128	128
HTS thin film@77 K	6″	0.275	1320	11.52	890	

Table 2. Quality factor and coil resistance comparison (outside the magnet).

Tuned at 8.92 MHz (outside magnet)						
Coil type/ temperature	Diameter (inch)	Inductance L (μH)	Unloaded Q	Coil resistance R_c (mΩ)	Loaded Q (phantom)	Loaded Q (wrist)
HTS tape@77 K	5″	0.31	2 300	7.5	1830	1330
Cu@77 K	5″	0.32	272	65.9	266	254
Ag@77 K	5″	0.31	174	100.5	163	159
Cu@300 K	5″	0.25	135	132.8	130	130
HTS thin film@77 K	6″	0.275	14 000	1.1		

The Q of the six-inch YBCO thin film surface coil also drops significantly from 14 000 to 1320 when placed inside the magnet. If we assume that the pre-amplifier loss is negligible, the sample resistance accounts for only 1.6% to 3.2% of the coil. As the sample loss does not dominate the noise content, the SNR should be improved through the use of the HTS tape coil.

4.2. Phantom imaging results

Phantom images were acquired with the HTS tape coil (77 K) and the six-inch YBCO thin film surface coil (77 K). Figure 4 shows the position of the RF coil and sample inside the magnet. Figure 5 shows the image comparison for the HTS thin film coil and HTS tape coil. The FOV enhancement produced by the volumetric HTS tape coil over the HTS film surface coil is clearly demonstrated.

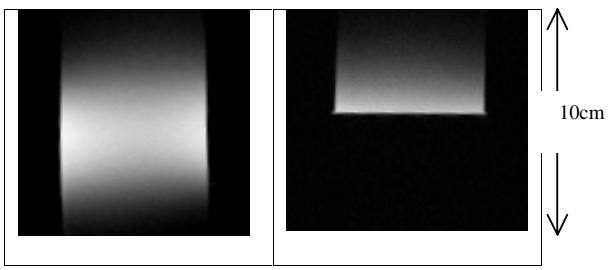

Figure 5. Phantom image comparison of the HTS tape coil (left) and YBCO thin film surface coil (right).

4.3. SNR profile

Figure 6 shows the SNR profile of each coil along the central axis. All the coils were also placed at the iso-centre of the magnet (i.e. depth = 0 mm). From figure 6, we observe

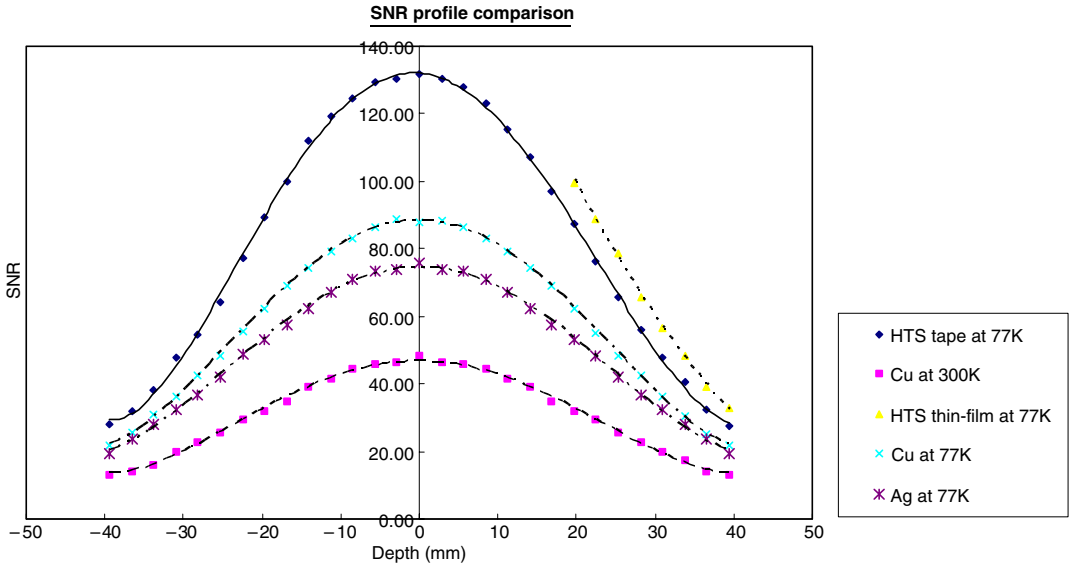

Figure 6. SNR profile comparison of HTS tape, copper coil, silver coil and HTS thin film surface coil.

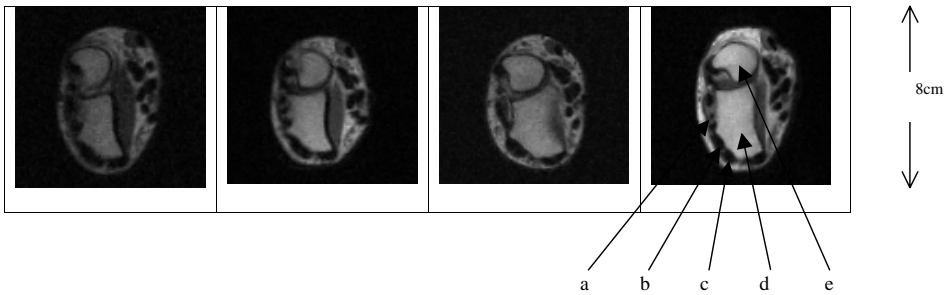

Figure 7. Axial image comparison for a human wrist (from left to right: copper coil, cool copper coil, cool silver coil, HTS tape coil).

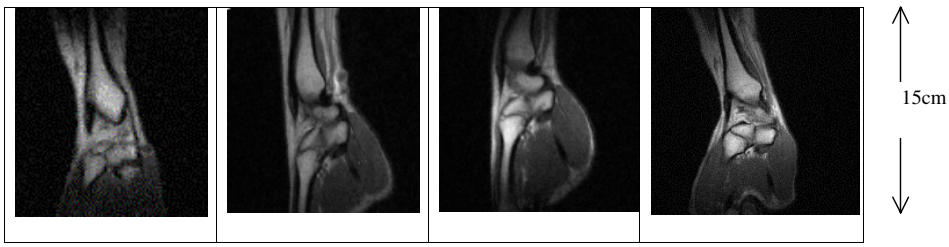

Figure 8. Coronal image comparison for a human wrist (from left to right: copper coil, cool copper coil, cool silver coil, Bi-2223 HTS tape coil).

that within ±2 cm from the iso-centre, the experimental (theoretical) SNR gains over the room temperature copper coil, the cool silver coil and the cool copper coil were about 260% (391%), 161% (204%) and 140% (165%) respectively. The discrepancy can be attributed to the effect of system noise to RF coil with different sensitivity (Q value).

In the theoretical prediction, the system noise contributed by the pre-amplifier, console and coaxial cable are neglected. This assumption works well for common metallic RF coil, which itself bears a substantial amount of noise. However, for the low loss HTS coil, the effect of system noise can be substantial. Therefore, the theoretical prediction is more accurate if the sensitivity of the two coils does not differ significantly.

4.4. Human imaging results

Figures 7 and 8 show axial and coronal images of the human wrist, respectively, which were acquired with various coils at 77 and 300 K. From figure 7, we can appreciate the benefit of the high SNR. From the HTS tape coil image, more soft tissue details and bone structure of the wrist can be identified (e.g. a: Pollicis Lonqus tendon; b: Extensor Carpi Radialis Brevis tendon; c: Extensor Carpi Radialis Lonqes tendon;

Table 3. Quality factor comparison on contact resistance.

	Q values (outside magnet)	
Coil type	Unloaded	Coil resistance (mΩ)
Original at 77 K	2300	7.5
Coil A at 77 K	1700	10.2
Coil B at 77 K	1050	16.5

d: radius and e: ulna). Clinically, human wrist images of higher resolution allow more accurate diagnosis of bone fracture and wrist trauma [16]. The SNR gain in the radius and ulna region is similar to the phantom imaging result.

4.5. Discussion

In addition to the enhanced FOV and simple fabrication process, another important advantage of the HTS tape coil is flexibility as regards size and configuration, which gives it great potential for use in building HTS volume coils. Therefore, it should be an attractive option for enhancing the SNR in low field systems. However, it should be pointed out that the technical challenges behind constructing HTS tape coils with more complex configurations are nontrivial. One of the major problems is the additional electrical contacts between segments of HTS tape and the capacitors.

Field homogeneity is an important benchmark in evaluating the quality of an RF coil. Coils with a homogeneous field configuration can improve the SNR over the entire FOV. Therefore, it is essential to design and optimize all kinds of volume coils with different shapes (e.g. solenoid, saddle or birdcage). However, RF coils with more complicated configurations come with additional electrical contacts. Our HTS tape coil is realized by normal soldering. To estimate the effect of contact resistance, we assembled two additional HTS tape coils (i.e. coil A and B), which have identical size and the same shape as the HTS tape coil that we used in collecting images. The only difference is that we have intentionally introduced one additional tape–tape joint on coil A and two additional tape–tape joints on coil B, in addition to the fundamental tape–capacitor joint. By measuring their natural resonant frequency, unloaded Q outside the magnet, and using equations (4) and (6), the tape–tape contact resistance is estimated. The results are summarized in table 3.

We have observed that the tape–tape joint resistance does not increase in proportion. One of the main reasons is that the dimension of the solder joint applied in the join was not identical. Also, the etched HTS tape and the solder material obviously exhibit different mechanical properties. When the coil was immersed in LN_2, the two materials contracted differently and introduced cracks in the HTS filaments. Although the data cannot be treated as final and conclusive, we have observed that the contact resistance of normal soldering is definitely nontrivial for the low loss HTS coil. Definitely, better controls on the above factors are essential for creating high quality volume coils. Therefore, our further work is on developing a low RF loss tape–tape and tape–capacitor interface with good mechanical properties for building volume coils. Possible applications include open coils (planar HTS surface coils) for interventional MR or close (volume) coil configurations dedicated to sports medicine.

5. Conclusion

We proposed a simpler and easier method for designing and fabricating HTS coils. Using industrial silver alloy sheathed $Bi_{(2-x)}Pb_xSr_2Ca_2Cu_3O_{10}$ (Bi-2223) HTS tapes, a five-inch single-turn HTS solenoid coil has been developed. Phantom and human wrist images have been acquired. The HTS tape coil has demonstrated an enhanced FOV over a six-inch YBCO thin film surface coil at 77 K with comparable SNR. In addition, the HTS tape coil at 77 K has achieved an average signal-to-noise ratio (SNR) improvement of (1) 260% over an equivalent copper coil at 300 K; (2) 140% over an equivalent copper coil at 77 K; and (3) 161% over an equivalent silver coil at 77 K.

Acknowledgments

We wish to thank the Chemistry and the Physics Department of the University of Hong Kong and Dr Murray Presland from Industrial Research Ltd, New Zealand, for their generous support.

References

[1] Black R D, Roemer P B and Mueller O M 1993 A high-temperature superconducting receiver for nuclear magnetic resonance microscopy *Science* **259** 793–5
[2] Ginefri J-C *et al* 2001 High temperature superconducting surface coil for *in vivo* microimaging of the human skin *Magn. Reson. Med.* **45** 376–82
[3] Black R D, Roemer P B and Mueller O M 1994 Electronics for a high temperature superconducting receiver system for magnetic resonance microimaging *IEEE Trans. Biomed. Eng.* **41** 195–7
[4] van Heteren J G *et al* 1994 Thin film HTS RF coil for low field MRI *Magn. Reson. Med.* **32** 396–400
[5] Ma Q Y *et al* 1999 Superconducting MR surface coils for human imaging *Proc. Magn. Reson. Med. Philadelphia, USA* 171
[6] Lee K H, Cheng M C, Chan K C, Wong K K, Yeung S S M, Lee K C, Ma Q Y and Yang E S 2004 Performance of large-size superconducting coil in 0.21 T MRI system *IEEE Trans. Biomed. Eng.* **51** 2024–30
[7] Ma Q Y 1999 RF applications of high temperature superconductors in MHz range *IEEE Trans. Appl. Supercond.* **9** 3565–8
[8] Haase A *et al* 1984 The influence of experimental parameters in surface-coil NMR *J. Magn. Reson.* **56** 401–2
[9] Hill H D W *et al* 1997 Improved sensitivity of NMR spectroscopy probes by use of high temperature superconductive detection coils *IEEE Trans. Appl. Supercond.* **7** 3750–5
[10] Smith D G, Gerner P S and Zuhoski C P 1997 A study of the applicability of high temperature superconducting rf receiver coils to the MRI industry *IEEE Trans. Appl. Supercond.* **7** 3710–4
[11] Kamisada Y, Koizumi T, Satou M and Yamada Y 1994 R&D of Ag-sheathed Bi-2223 superconducting tapes *IEEE Trans. Magn.* **30** 1675–80
[12] http://www.amsuper.com/html/products/library/002-MultiFactFS01-02.pdf
[13] Ginefri J-C *et al* 1999 Quick measurement of NMR coil sensitivity with a single-loop probe *Rev. Sci. Instrum.* **70** 4730–1
[14] Balachandran *et al* 1999 Method and etchant to join Ag-clad BSSCO superconducting tape *US Patent Specification* No 5,882,536
[15] Bohn C L, Delayen J R, Dos Santos D I, Lanagan M T and Shepard K W 1989 RF properties of high-Tc superconductors *IEEE Trans. Magn.* **25** 2406–9
[16] Mack M G *et al* 2003 Clinical impact of MRI in acute wrist fractures *Eur. Radiol.* **13** 612–7